Susceptibility corrections in solid state NMR experiments with oriented membrane samples. Part II: Theory

Reinhard Ulrich,[a] Ralf W. Glaser,[b] and Anne S. Ulrich[c,*]

[a] *Technische Universitaet Hamburg-Harburg, Hamburg D-21071, Germany*
[b] *Institute of Molecular Biology, Friedrich-Schiller-Universitaet, Winzerlaer Str. 10, Jena D-07745, Germany*
[c] *Forschungszentrum Karlsruhe, IFIA, POB 3640, Karlsruhe D-76021/76131, Germany*

Abstract

In solid state NMR analysis of oriented biomembranes the samples typically have the shape of a rectangular block, formed by stacking a number of glass slides coated with the membranes under investigation. Reference material may be provided internally in the volume of the block or as an external layer on its surface, as described in the accompanying paper [J. Magn. Reson. 164 (2003) 104–114]. The demagnetizing field resulting in such non-spheroidal samples is inhomogeneous. It shifts and broadens the NMR lines of both the sample and of the reference, as compared to the ideal of a spherical sample. The magnitude of these effects is typically of the order of a few ppm. To determine the necessary corrections, a general analysis is presented here for the demagnetizing field of a layered sample of rectangular block geometry, with the normal of the layers parallel to the main field or tilted about an axis of the block. The correction to the line position of the block sample is found to be approximately equal to that of the spheroid which can be inscribed into the block, and for which the correction is well known. For an external reference layer, placed on top of the block, the correction can be found by the same approximation, invoking a simple mirror concept. The layered structure of the block can be accounted for by using an average magnetic susceptibility. Sample and support materials contribute to that average according to their volume filling factors. If the sample material is anisotropic at the molecular level, as e.g. lipid bilayers are, the resulting anisotropy of the block is reduced by the filling factor of the sample material.
© 2003 Elsevier Inc. All rights reserved.

Keywords: Chemical shift reference; Bulk magnetic susceptibility effects; Inhomogeneous line broadening; Lipid membranes

1. Introduction

When a sample is inserted into the magnetic field of an NMR spectrometer, a 'demagnetizing field' is induced in the sample, depending on its susceptibility, shape, internal structure, and orientation. The influence of this field on the precession frequency of a spin in the sample is a classic problem of NMR spectroscopy, referred to as bulk magnetic susceptibility (BMS) effect. It is absent only in homogeneous spherical samples. In spheroidal samples it causes a shift of the NMR lines, in samples of more general shapes also line broadening

results. These effects are analyzed here because they are essential in referencing NMR measurements of macroscopically oriented lipid membranes [1]. Previously, BMS effects have received special attention in high resolution NMR [2–4] and in NMR imaging of heterogeneous or compartmentalized structures, such as biological tissues and trabecular bones [5–7]. The BMS-induced line broadening can be reduced by shimming, as recently demonstrated by Soubias et al. [8] in a cylindrical sample of stacked membranes.

The samples of interest are prepared by depositing lipid bilayers on thin glass slides and then stacking many of those to form a layered block [1,9], like a deck of cards, see Fig. 1a. For calibration, reference material has to be provided. Preferably it should occupy the same volume as the sample material and should have a sharp line not overlapping with the spectrum of the
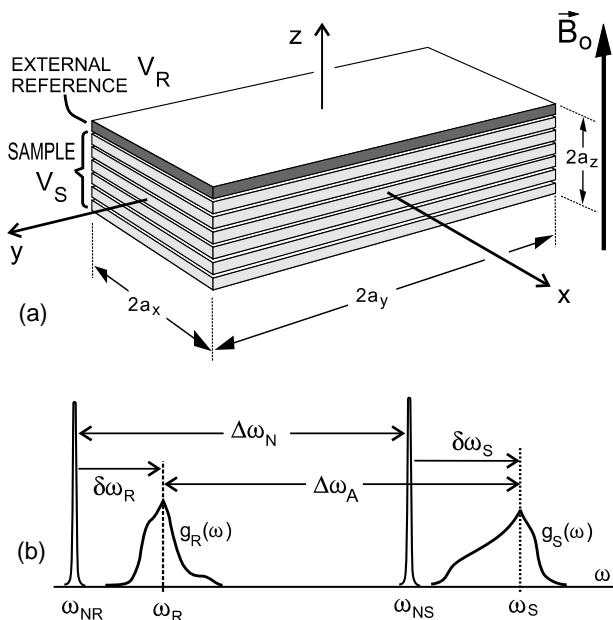
Fig. 1. (a) Block shaped sample, formed by stacking a number of glass slides coated with lipid membranes. An external reference layer may be attached on top of the stack. (b) The inhomogeneous demagnetizing field causes a shift and broadening of the NMR lineshapes $g_S(\omega)$ and $g_R(\omega)$ of both sample and reference.

membranes. When such an *internal* reference is impractical, an *external* reference slab may be attached to the top of the sample stack, forming another compartment there [1].

These experimental situations must be compared with the ideal case of a spherical sample, throughout which the field is homogeneous. Here, a narrow line would be observed of the nominal frequency $\omega_{N,S}$, characteristic of the spin under investigation and its environment. A reference spin, likewise, would produce a narrow line of frequency $\omega_{N,R}$ if the reference material were spherical. Their difference $\Delta\omega_N$ is the nominal chemical shift of the sample spin relative to the reference spin, used traditionally in NMR spectroscopy

$$\Delta\omega_N = \omega_{N,S} - \omega_{N,R}. \tag{1}$$

In the block-shaped sample, however, the demagnetizing field is inhomogeneous, and the Larmor frequency of the spin under investigation depends on its position $\mathbf{r}$ in the sample compartment. Therefore, an inhomogeneously broadened line of frequency distribution $g_S(\omega)$ results rather than the sharp resonance at $\omega_{N,S}$, see Fig. 1b. Likewise, a broadened reference line $g_R(\omega)$ is measured instead of the sharp peak at $\omega_{N,R}$. If we characterize the broadened lines $g_S(\omega)$ and $g_R(\omega)$ by suitably chosen dominant frequencies ω_S and ω_R, we can define line shifts $\delta\omega_S$ and $\delta\omega_R$ of sample and reference, respectively. Using them, the chemical shift $\Delta\omega_N$ may be expressed by the 'apparent' chemical shift $\Delta\omega_A = \omega_S - \omega_R$ of the measurement and two correction terms

$$\delta\omega_S = \omega_S - \omega_{N,S},$$
$$\delta\omega_R = \omega_R - \omega_{N,R},$$
$$\Delta\omega_N = \Delta\omega_A - \delta\omega_S + \delta\omega_R. \tag{2}$$

It is the purpose of this paper to determine these correction terms, $\delta\omega_S$ and $\delta\omega_R$, and to discuss their dependence on the shape, orientation, and layered structure of the stacked sample block, and of an external reference layer. In particular, we want to find the influence which the demagnetizing field of the sample compartment has on the reference compartment, i.e., on $\delta\omega_R$.

To analyze these BMS effects, we start in Section 2 by outlining the theoretical background. The demagnetizing field of a block-shaped sample is calculated from its magnetization. The spatial distributions of the magnetic fields $\mathbf{H}(\mathbf{r})$ and $\mathbf{B}(\mathbf{r})$ are determined. They can be used to derive the lineshape $g(\omega)$ for any selected compartment. By this formalism BMS *volume* effects in block-shaped samples are discussed in Section 3. A quantitative understanding of BMS *surface* effects is required for external referencing. Section 4 explains a 'mirror' scheme which allows to express these surface effects in terms of the bulk effects derived before. Up to that point we treat the sample block as homogeneous, ignoring the layered structure of the stack. Then, in Section 5, we take the layers into account by interpreting the layered block as an 'artificial magnetic material,' characterized by an average susceptibility. This permits calculation of the actual fields in the membranes, yielding another small correction.

2. Theoretical background

Fundamentals. To derive the field $\mathbf{B}(\mathbf{r})$ at the site $\mathbf{r}$ of a nuclear spin in a sample, it is convenient [4,6] to define a small ficticious *Lorentz sphere* of radius R_L around $\mathbf{r}$, see Fig. 2a. It is chosen large compared to interatomic distances, thus containing a representative number of neighboring atoms. The *near field* $\mathbf{H}^{(N)}(\mathbf{r})$ is produced at $\mathbf{r}$ by the arrangement of all discrete magnetic moments in the neighborhood of $\mathbf{r}$. If there were no magnetic moments outside the Lorentz sphere and if all other effects of line shift and broadening are ignored, the Larmor frequency of the spin at $\mathbf{r}$ would be $\omega_N(\mathbf{r}) = \gamma |\mathbf{B}^{(N)}(\mathbf{r})|$, where $\mathbf{B}^{(N)}(\mathbf{r}) = \mu_o(\mathbf{H}^{(o)} + \mathbf{H}^{(N)}(\mathbf{r}))$ results from the superposition of the near field $\mathbf{H}^{(N)}(\mathbf{r})$ and the main field $\mathbf{H}^{(o)}$ of the NMR magnet. Here, γ is the gyromagnetic ratio of the nucleus at $\mathbf{r}$, and μ_o the permeability of free space. This frequency $\omega_N(\mathbf{r})$ is the quantity of primary interest in NMR spectroscopy because it is characteristic of the neighborhood of $\mathbf{r}$.

Magnetic moments outside the Lorentz sphere V_L produce an additional field $\mathbf{H}^{(BMS)}(\mathbf{r})$ at $\mathbf{r}$ that modifies
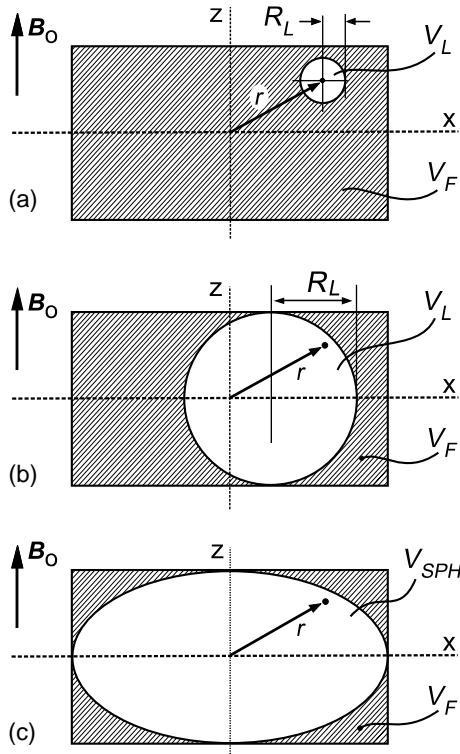
Fig. 2. (a) Around a spin at point $\mathbf{r}$ a small 'Lorentz sphere' is defined. Magnetic moments inside are dealt with individually, those outside by continuum theory. (b) The material inside a large spherical shell, containing the spin at $\mathbf{r}$, produces no BMS effects at $\mathbf{r}$. Only material outside (hatched) causes a BMS related line shift and broadening. (c) A shell in the form of a spheroid V_{SPH} produces a predictable shift. The material outside causes an additional inhomogeneous shift and broadening.

the Larmor frequency. This is the BMS effect. Because the distance of those spins from $\mathbf{r}$ is large on an interatomic scale, $\mathbf{H}^{(BMS)}(\mathbf{r})$ may be calculated by continuum theory. Accordingly, the source of $\mathbf{H}^{(BMS)}(\mathbf{r})$ is the bulk magnetization $\mathbf{M}(\mathbf{r})$ of the material outside V_L. That 'far' volume (hatched in Fig. 2) is denoted by V_F. All volume elements dV' at positions $\mathbf{r}'$ in V_F act as elementary dipole moments $\mathbf{M}(\mathbf{r}')dV'$, producing jointly the field

$$\mathbf{H}^{(BMS)}(\mathbf{r}) = \frac{1}{4\pi} \iiint\limits_{(V_F)} [3(\mathbf{M}(\mathbf{r}')\mathbf{R})\mathbf{R} \\ - \mathbf{M}(\mathbf{r}')\mathbf{R}^2]|\mathbf{R}|^{-5}dV'. \quad (3)$$

Here, the vector $\mathbf{R} = \mathbf{r} - \mathbf{r}'$ extends from the position $\mathbf{r}'$ of dV' to the point $\mathbf{r}$ of interest. As the Lorentz sphere has been cut out of the sample, the singularity of the integrand in Eq. (3) at $\mathbf{R} \to 0$ poses no problem. Actually, despite that singularity the integral (3) has a definite value even if it is extended over the entire sample volume V_S or over the Lorentz volume V_L. This can be recognized by converting the volume integral (3) into a surface integral (see below). As the singularity is identical in both cases (V_S, V_L) it is possible to rewrite the BMS field

as the difference $\mathbf{H}^{(BMS)} = \mathbf{H}^{(S)} - \mathbf{H}^{(L)}$ of two fields $\mathbf{H}^{(S)}(\mathbf{r})$ and $\mathbf{H}^{(L)}(\mathbf{r})$ which are given by expressions like Eq. (3). For $\mathbf{H}^{(S)}(\mathbf{r})$ the integration runs over the entire sample volume V_S,

$$\mathbf{H}^{(S)}(\mathbf{r}) = \frac{1}{4\pi} \iiint\limits_{(V_S)} [3(\mathbf{M}(\mathbf{r}')\mathbf{R})\mathbf{R} - \mathbf{M}(\mathbf{r}')\mathbf{R}^2]|\mathbf{R}|^{-5}dV'. \quad (4)$$

For $\mathbf{H}^{(L)}(\mathbf{r})$ an identical expression holds, with integration over the Lorentz sphere V_L. These fields $\mathbf{H}^{(S)}(\mathbf{r})$ and $\mathbf{H}^{(L)}(\mathbf{r})$ are known in magnetostatics as the *demagnetizing fields*. Using them, the total field at the site of interest can be expressed as

$$\mathbf{H}(\mathbf{r}) = \mathbf{H}^{(o)} + \mathbf{H}^{(N)}(\mathbf{r}) + \mathbf{H}^{(BMS)}(\mathbf{r}) \\ = \mathbf{H}^{(o)} + \mathbf{H}^{(N)}(\mathbf{r}) + \mathbf{H}^{(S)}(\mathbf{r}) - \mathbf{H}^{(L)}(\mathbf{r}). \quad (5)$$

The source of the demagnetizing fields is the magnetization $\mathbf{M}(\mathbf{r})$. It is induced by the local flux density according to the local magnetic susceptibility $\chi(\mathbf{r})$, which may be a tensor if the material is anisotropic

$$\mathbf{M}(\mathbf{r}) = \chi(\mathbf{r})\mathbf{B}(\mathbf{r})/\mu_o = \chi(\mathbf{r})[1 + \chi(\mathbf{r})]\mathbf{H}(\mathbf{r}). \quad (6)$$

As $\mathbf{M}(\mathbf{r})$ is determined by $\mathbf{H}(\mathbf{r})$ and, conversely, $\mathbf{H}(\mathbf{r})$ depends on $\mathbf{M}(\mathbf{r})$, it would generally be necessary to find $\mathbf{H}(\mathbf{r})$ and $\mathbf{M}(\mathbf{r})$ for a given $\chi(\mathbf{r})$ as a simultaneous solution of Eqs. (5) and (6). For NMR samples, however, the calculation of $\mathbf{H}(\mathbf{r})$ and $\mathbf{M}(\mathbf{r})$ is simplified because typically $|\chi| < 10^{-5}$. Therefore, the three terms $\mathbf{H}^{(N)}(\mathbf{r})$, $\mathbf{H}^{(S)}(\mathbf{r})$, and $\mathbf{H}^{(L)}(\mathbf{r})$ in Eq. (5) are only small perturbations to the main field $\mathbf{H}^{(o)}$ and may be neglected in the calculation of $\mathbf{M}$. The relative error incurring this way in $\mathbf{M}$ is only of the order of $|\chi| \approx 10^{-5}$ (corresponding to $\approx 10^{-4}$ ppm of chemical shift) and may well be ignored. We characterize the direction of the main field $\mathbf{H}^{(o)} = H_o\mathbf{h}^{(o)}$ by a unit vector $\mathbf{h}^{(o)}$ and obtain

$$\mathbf{M}(\mathbf{r}) \approx \chi(\mathbf{r})\mathbf{H}^{(o)}(\mathbf{r}) = H_o\chi(\mathbf{r})\mathbf{h}^{(o)}. \quad (7)$$

For a general sample the demagnetizing field Eq. (4) can now be expressed as

$$\mathbf{H}^{(S)}(\mathbf{r}) = -\hat{\mathcal{D}}(\mathbf{r})\mathbf{M}(\mathbf{r}) = -\hat{\mathcal{D}}(\mathbf{r})\chi(\mathbf{r})\mathbf{H}^{(o)}(\mathbf{r}) \\ = -H_o\mathcal{D}(\mathbf{r})\chi(\mathbf{r})\mathbf{h}^{(o)}, \quad (8)$$

where $\hat{\mathcal{D}}(\mathbf{r})$ is the normalized local demagnetization tensor of V_S [4]. Its components are

$$\mathcal{D}_{ij}(\mathbf{r}) = \frac{1}{4\pi} \iiint\limits_{(V_S)} [3R_iR_j - \mathbf{R}^2\delta_{ij}]|\mathbf{R}|^{-5}dV. \quad (9)$$

At any point $\mathbf{r}$ inside or outside V_S Eq. (8) assigns $-\hat{\mathcal{D}}(\mathbf{r})\chi(\mathbf{r})\mathbf{H}^{(o)}$ as the demagnetizing field $\mathbf{H}^{(S)}(\mathbf{r})$ to the given main field $\mathbf{H}^{(o)}$. In components, $H_i^{(S)}(\mathbf{r}) = -\sum_j \sum_k \mathcal{D}_{ij}(\mathbf{r})\chi_{jk}(\mathbf{r})h_k^{(o)}$ for $i, j, k = \{x, y, z\}$. Definition (9) shows that $\mathcal{D}(\mathbf{r})$ is a purely geometrical function, depending only on the shape of V_S. It is symmetric in i, j. Its eigenvectors represent those directions of $\mathbf{h}^{(o)}$ for which $\mathbf{M}(\mathbf{r})$ is parallel to $\mathbf{h}^{(o)}$. The associated eigenvalues $\mathcal{D}_{ii}(\mathbf{r})$ obey the sum rule [10]

$$\mathrm{Tr}[\hat{\mathcal{D}}(\mathbf{r})] = \mathcal{D}_{11}(\mathbf{r}) + \mathcal{D}_{22}(\mathbf{r}) + \mathcal{D}_{33}(\mathbf{r}) = 1. \tag{10}$$

For a spherical sample symmetry requires $\mathcal{D}_{11}(\mathbf{r}) = \mathcal{D}_{22}(\mathbf{r}) = \mathcal{D}_{33}(\mathbf{r}) = 1/3$ and $\hat{\mathcal{D}}$ becomes scalar, and the demagnetizing field of the Lorentz sphere in a material with homogeneous χ is

$$\mathbf{H}^{(L)} = -\chi \mathbf{H}^{(o)}/3. \tag{11}$$

The Larmor frequency $\omega(\mathbf{r})$ of a spin at position $\mathbf{r}$ is determined by the magnitude of the local field, $\omega(\mathbf{r}) = \gamma|\mathbf{B}(\mathbf{r})|$. Compared to the frequency $\omega_N = \gamma\mu_o|\mathbf{H}^{(o)} + \mathbf{H}^{(N)}|$ of a spin free of BMS effects, the frequency in a general sample is offset by $\delta\omega(\mathbf{r}) = \omega(\mathbf{r}) - \omega_N = \gamma\delta|\mathbf{B}(\mathbf{r})|$, where $\delta|\mathbf{B}(\mathbf{r})| = |\mathbf{B}(\mathbf{r})| - |\mathbf{B}^{(N)}(\mathbf{r})|$ is the modification produced by the BMS field Eq. (3) in the vacuum representation. This offset is found by evaluating $\delta|\mathbf{B}^2| = \mathbf{B}^2 - \mathbf{B}^{(N)2} = 2|\mathbf{B}|\delta|\mathbf{B}| = 2\mu_o\mathbf{B}^{(N)}\mathbf{H}^{(\mathrm{BMS})}$. We assume now that the susceptibility χ is isotropic. Neglecting terms of order χ^2 and higher

$$\begin{aligned}\delta\omega(\mathbf{r})/\omega_N &= \delta|\mathbf{B}(\mathbf{r})|/B^{(o)} \\ &= \mathbf{H}^{(o)}[\mathbf{H}^{(S)}(\mathbf{r}) - \mathbf{H}^{(L)}(\mathbf{r})]/H_o^2. \end{aligned} \tag{12}$$

Consequently, BMS effects result only from that component of the demagnetizing field $\mathbf{H}^{(S)}(\mathbf{r})$ which is parallel to the main field $\mathbf{H}^{(o)}$. Inserting here Eqs. (3) and (11) we find the BMS shift, normalized to $\chi\omega_N$

$$\frac{\delta\omega(\mathbf{r})}{\chi\omega_N} = \frac{\delta|\mathbf{B}(\mathbf{r})|}{\chi B^{(o)}} = \frac{1}{3} - \mathbf{h}^{(o)}\hat{\mathcal{D}}(\mathbf{r})\mathbf{h}^{(o)} = \frac{1}{3} - \mathcal{D}_{hh}(\mathbf{r}). \tag{13}$$

Here, $\mathcal{D}_{hh}(\mathbf{r}) = \mathbf{h}^{(o)}\hat{\mathcal{D}}(\mathbf{r})\mathbf{h}^{(o)}$ is the component of $\hat{\mathcal{D}}(\mathbf{r})$ along the direction $\mathbf{h}^{(o)}$ of the main field. If the sample is oriented with its z axis (unit vector $\mathbf{z}^o$) along the main field, Eq. (13) simplifies,

$$\frac{\delta\omega(\mathbf{r})}{\chi\omega_N} = \frac{\delta|\mathbf{B}(\mathbf{r})|}{\chi B^{(o)}} = \frac{1}{3} - \mathcal{D}_{zz}(\mathbf{r}), \tag{14}$$

where

$$\mathcal{D}_{zz}(\mathbf{r}) = \frac{1}{4\pi}\iiint\limits_{(V_S)}[3(\mathbf{R}\mathbf{z}^o)\mathbf{R} - |\mathbf{R}|^2\mathbf{z}^o]|\mathbf{R}|^{-5}\,\mathrm{d}V'. \tag{15}$$

Eqs. (13) and (14) are compact formulations of the general BMS effect of homogeneous samples. The shape and orientation of the sample volume V_S determine the demagnetization function $\mathcal{D}_{hh}(\mathbf{r})$ which, in turn, governs the local modification $\delta\omega(\mathbf{r})$ of the precession frequency. At such points $\mathbf{r}$ in the sample where $\mathcal{D}_{hh} = 1/3$, the modification vanishes, $\delta\omega(\mathbf{r}) = 0$. This situation exists, for example, throughout a spherical sample or, by symmetry and Eq. (10), at the center of a cube. At other points the deviation of $\mathcal{D}_{hh}$ from this special value $1/3$ gives directly the BMS modification of the normalized precession frequency. In the typical diamagnetic case ($\chi < 0$), the modification is positive ($\delta\omega > 0$ or $\delta B > 0$) when $\mathcal{D}_{zz} > 1/3$. In spectroscopists' jargon this is a 'downfield' shift.

An alternative formulation of the BMS field helps to clarify the properties of $\mathbf{H}^{(\mathrm{BMS})}(\mathbf{r})$ and simplifies numerical calculations of $\hat{\mathcal{D}}(\mathbf{r})$. It is based on the scalar magnetic potential $\varphi(\mathbf{r})$ by which the demagnetizing field can be expressed as $\mathbf{H}^{(S)}(\mathbf{r}) = -\mathrm{grad}\varphi(\mathbf{r})$. The sources of φ follow from $\mathrm{div}\mathbf{B}(\mathbf{r}) = 0$. As $\mathbf{H}^{(S)}(\mathbf{r})$ is a smoothly varying field, continuum theory applies, and the average $\langle\mathbf{H}^{(N)}(\mathbf{r}) + \mathbf{H}^{(L)}(\mathbf{r})\rangle = 0$ vanishes over V_L. Therefore, $\mathbf{B}(\mathbf{r}) = \mu_o(\mathbf{H}^{(o)} + \mathbf{H}^{(S)}(\mathbf{r}) + \mathbf{M}(\mathbf{r}))$ and, neglecting terms of higher order in χ,

$$\mathrm{div}\mathbf{H}^{(S)}(\mathbf{r}) = -\mathrm{div}\mathbf{M}(\mathbf{r}) \approx -\mathbf{H}^{(o)}(\mathbf{r})\mathrm{grad}\chi(\mathbf{r}). \tag{16}$$

With homogeneous samples the sources of the demagnetizing field are ficticious 'magnetic charges' at the discontinuities of $\chi(\mathbf{r})$, on the surface of the sample. According to this well known concept, a magnetic charge density $\sigma(\mathbf{r}) = \chi H_o\mathbf{a}_n^o\mathbf{h}^{(o)} = \chi H_o\cos\eta_h(\mathbf{r})$ may be postulated to exist on the surface A_S of the sample. This $\sigma(\mathbf{r})$ generates the magnetic field $\mathbf{H}^{(S)}(\mathbf{r})$ in the same way as electric charges would generate an electric field. Here, $\mathbf{a}_n^o$ is the outward normal unit vector of the sample volume, and $\eta_h(\mathbf{r})$ is the angle between $\mathbf{a}_n^o$ and $\mathbf{h}^{(o)}$. The potential $\varphi(\mathbf{r})$ of the surface charges $\sigma(\mathbf{r}')$ is found by integration over all surface elements $\mathrm{d}\mathbf{A}' = \mathbf{a}^o\,\mathrm{d}A'$. The demagnetization tensor then follows by the *gradient* operation

$$\frac{\varphi(\mathbf{r})}{\chi\mathbf{H}_o} = \frac{1}{4\pi}\iint\limits_{(A_S)}\frac{\mathbf{h}^{(o)}\mathrm{d}\mathbf{A}'}{|\mathbf{R}|} = \frac{1}{4\pi}\iint\limits_{(A_S)}\frac{\cos\eta_h(\mathbf{r}')\mathrm{d}A'}{|\mathbf{R}|}, \tag{17}$$

$$\mathcal{D}_{ij}(\mathbf{r}) = \frac{1}{4\pi}\iint\limits_{(A_S)}|\mathbf{R}|^{-3}R_i\,\mathrm{d}A_j'. \tag{18}$$

This is an alternative formulation of $\mathcal{D}_{ij}(\mathbf{r})$. As the integrations in Eqs. (17) and (18) extend over the surface of the sample, the integrands are regular at all points $\mathbf{r}$ inside the sample. Consequently, in Eqs. (4) and (9) the singularity at $|\mathbf{R}| \to 0$ does not affect the integration. This justifies the decomposition of the BMS field into the two demagnetizing fields $\mathbf{H}^{(S)}(\mathbf{r})$ and $\mathbf{H}^{(L)}(\mathbf{r})$ which had been introduced in Eq. (5).

3. BMS volume effects

Spheroidal samples. Although we are interested in layered block-shaped samples, we start by considering samples which have the shape of a general spheroid with homogeneous susceptibility ($\chi = \mathrm{const}$). A *spheroid*, in this context, is a sphere 'stretched' by individual factors along three orthogonal axes. When two of the stretching factors are equal, an ellipsoid of revolution results. The intersection of a spheroid with any plane is an ellipse. Samples having the shape of such spheroids will serve later on for comparison with the block-shaped samples. It is well known [11] that inside a spheroid, placed into a homogeneous field $\mathbf{B}^{(o)}$, both the magnetization $\mathbf{M}$ and

the demagnetizing field $\mathbf{H}^{(S)} = -\hat{\mathcal{D}}\mathbf{M}$ are homogeneous, and $\hat{\mathcal{D}}$ and ω are independent of position $\mathbf{r}$. The spectrum is a narrow line, therefore. Its frequency is determined by $\mathcal{D}_{hh}$ according to Eq. (13) and depends on the orientation of the spheroid. Generally the direction of $\mathbf{H}^{(S)}$ is not parallel to $\mathbf{M}$, because $\hat{\mathcal{D}}$ is a tensor. Only when the sample is oriented with one of its principal axes ($i = x, y, z$) along the main field $\mathbf{B}^{(o)}$, the parallelism exists and

$$\mathcal{D}_{zz}(\mathbf{r}) = \frac{\text{local demagnetizing field } |H_z^{(S)}(\mathbf{r})| \text{ at position } \mathbf{r} \text{ in sample}}{\text{uniform demagnetizing field } |H_z^{(S)}| \text{ in an infinite slab-shaped sample}}.$$

$$\mathbf{H}^{(S)} = -D_i \mathbf{M} \approx -\chi D_i \mathbf{B}^{(o)}/\mu_o. \tag{19}$$

The three eigenvalues $\mathcal{D}_{ii}$ are independent of position, too, and traditionally they are called the *demagnetizing factors* D_i of the spheroid. Accordingly, the sum rule Eq. (10) reads for a spheroid $\sum D_i = 1$. Assuming $\chi > 0$ (paramagnetic case) the negative signs in Eq. (19) indicate that $\mathbf{H}^{(S)}$ is directed opposite to the main field $\mathbf{H}^{(o)}$. This is the reason why $\mathbf{H}^{(S)}(\mathbf{r})$ is called the *demagnetizing field*. For a spheroid with semi-axes a_x, a_y, a_z, elementary theory [11] gives the demagnetization factors as definite integrals,

$$D_i(a_x, a_y, a_z) = \frac{a_x a_y a_z}{2} \int_0^{\infty} \frac{\mathrm{d}u}{(u + a_i^2)W(u)}, \tag{20}$$

where $W(u) = [(u + a_x^2)(u + a_y^2)(u + a_z^2)]^{1/2}$. Each D_i depends actually on only two variables, i.e., on two ratios of the three axes $\{a_x, a_y, a_z\}$. For a number of simple spheroids the D_i are listed in Table 1. Here, the shape of the spheroids is characterized by their aspect ratio $q = a_z/a_x$ and aspect angle $\alpha = \arctan(q)$. By varying $0 < q < \infty$ or, correspondingly, $0 < \alpha < 90°$, the widest possible range is covered.

For general spheroids the values of the D_i may be taken from published tables [12]. For practical usage it may be more convenient to compute the D_i by numerical evaluation of Eq. (20), using any standard integration routine [13–15] which replaces the integral (20) by a sum of e.g. 10^5 terms.

Two examples from Table 1 are of particular interest concerning block-shaped samples. One is the sphere already mentioned. The other one is the infinitely extended slab, the limiting form of an oblate spheroid, oriented normal to $\mathbf{H}^{(o)}$. Here, we have $D_z = 1$, and therefore $\mathbf{H}_z^{(S)} = -\chi H_o$. This result permits a general interpretation of the factor D_z and, more generally, of the function $\mathcal{D}_{zz}(\mathbf{r})$ as the ratio

For an ellipsoid of revolution ($a_x = a_y$ and $a_z = qa_x$) we have $D_x = D_y = (1 - D_z)/2$ and the demagnetizing factor D_z is [11]

$$D_z(q) = \frac{q \ln[q + \sqrt{q^2 - 1}]}{(q^2 - 1)^{3/2}} - \frac{1}{q^2 - 1}. \tag{21}$$

This expression evaluates to a real D_z for $q > 1$ as well as for $q < 1$. The dependence of D_z on the aspect angle $\alpha = \arctan(q)$ is illustrated in Fig. 3 at the right ordinate. The left ordinate gives the normalized frequency devia-
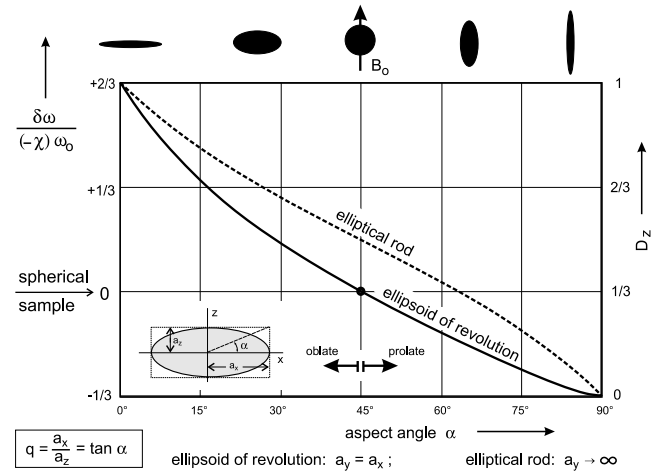

Fig. 3. Demagnetization factor $D_z(\alpha)$ of simple spheroidal samples with aspect angle $\alpha = \arctan(a_z/a_x)$ (right ordinate). The left ordinate gives the normalized frequency deviation for diamagnetic samples.

Table 1
Demagnetization factors of spheroids with semi-axes a_x, a_y, and $a_z = qa_x$

Spheroid	Axes	q	D_x	D_y	D_z
Infinite slab in xy plane	$a_x \to \infty$; $a_y \to \infty$	$= 0$	0	0	1
Thin circular disk in xy plane	$a_x = a_y$; $a_z \ll a_x$	$\ll 1$	$1 - D_z/2$	$1 - D_z/2$	$1 - q\pi/2$
Sphere	$a_x = a_y = a_z$	$= 1$	1/3	1/3	1/3
Elliptical rod along y axis	$a_y \to \infty$		$q/(q+1)$	0	$1/(q+1)$
Circular rod along y axis	$a_y \to \infty$; $a_z = a_x$	$= 1$	1/2	0	1/2
Long ellipsoid along z axis	$a_z \to \infty$; $a_y = a_x$	$\gg 1$	$1 - D_z/2$	$1 - D_z/2$	$(\ln 2q - 1)/q^2$

tion $\delta\omega$ for diamagnetic spheroids. A sample in the form of a flat spheriodal disk, with dimensions $a_x = a_y = 10$ mm and $a_z = 4.8$ mm and with the susceptibility of glass ($\chi \approx -12 \times 10^{-6}$), for example, has the aspect angle $\alpha \approx 30°$ and a demagnetization factor $D_z \approx 0.54$. A correction of $(-\chi)(D_z - 1/3) \approx +2.5$ ppm would have to be applied in the sense of Eq. (1) to any measured line to obtain the chemical shift.

Non-spheroidal samples have inhomogeneous demagnetizing fields $\mathbf{H}^{(S)}(\mathbf{r})$. Ignoring all other effects of line shift and broadening, the spatial distribution of the BMS related shift $\delta\omega(\mathbf{r})$ in the sample results in a lineshape

$$g_S(\omega - \omega_N)\,\mathrm{d}\omega = \frac{\chi\omega_N}{V_o} \iiint\limits_{[\mathbf{r}:\delta\omega(\mathbf{r})\in\mathrm{d}\omega]} S^2(\mathbf{r})\,\mathrm{d}V(\mathbf{r}). \qquad (22)$$

Here, ω_N is the frequency that would be measured with a spherical sample. The integration extends over all volume elements $\mathrm{d}V(\mathbf{r})$ of the sample which are situated at points $\mathbf{r}$ at which the local frequency offset $\delta\omega(\mathbf{r})$ falls in the interval $\omega \ldots (\omega + \mathrm{d}\omega)$. The contribution of any such volume element to the spectral density $g_S(\omega - \omega_N)$ is proportional to $\mathrm{d}V(\mathbf{r})$. Computationally, the determination of $g_S(\omega - \omega_N)$ is a sorting procedure, equivalent to the formation of a histogram [3,5]. A weighting function $S^2(\mathbf{r})$ may be included in Eq. (22) to take into account the spatial distribution of the excitation and detection sensitivities in the sample volume. The normalization factor V_o is a chosen so that $\int g_S(\omega - \omega_N)\,\mathrm{d}\omega = 1$.

For a qualitative understanding of the lineshape Eq. (22) of homogeneous samples of general shape we have a closer look at the role of the Lorentz sphere. According to our derivation, the origin of the inhomogeneity of $\mathbf{H}^{(S)}(\mathbf{r})$ is the magnetization outside the Lorentz sphere, indicated by the hatched area in Fig. 2a. The Lorentz sphere itself has a demagnetizing field $\mathbf{H}^{(L)} = -(\chi/3)\mathbf{H}^{(o)}$ which is independent of its radius R_L. It follows, therefore, that a spherical shell, concentric with the Lorentz sphere and contained entirely in the sample volume V_S, does not contribute to the demagnetizing field $\mathbf{H}^{(S)}(\mathbf{r})$. Such a shell causes no BMS related shift nor broadening of NMR lines. Therefore, the value of R_L chosen in defining the 'near field' $\mathbf{H}^{(N)}(\mathbf{r})$ is not critical. Actually, R_L may be increased up to the limit where the sphere touches the walls of the sample, as indicated in Fig. 2b, without affecting the demagnetizing field $\mathbf{H}^{(S)}(\mathbf{r})$.

One may try in this way to identify that volume V_F which is responsible for the BMS effects at a given $\mathbf{r}$ by cutting out of the sample the largest possible sphere containing $\mathbf{r}$. Inside that sphere inhomogeneity of $\mathbf{H}^{(S)}(\mathbf{r})$ results only from the outside volume elements. At the center of a cubic sample ($a_x = a_y = a_z = a$), for example, maximally a sphere of radius a can be cut out, leaving the eight corner sections as the sources of inhomogeneity.

Extending this procedure, spheroidal cut-outs may be considered instead of spheres, see Fig. 2c. If such a spheroidal 'core' itself were a sample, its internal field would be homogeneous, resulting in a sharp but shifted NMR line. The volume outside the core, however, adds inhomogeneity to the field, causing line broadening and, possibly, additional shift. For block-shaped samples these considerations suggest that the shift of the overall line should be roughly comparable to that of the inscribed spheroid. This expectation is confirmed by the calculations given below.

For *block-shaped samples* the distribution of demagnetization $\hat{\mathcal{D}}(\mathbf{r})$ can be found by performing the integration Eq. (15), using standard symbolic manipulation [13,14]. The simplest situation exists when the block is aligned with the field as shown in Fig. 1. In evaluating for this case the volume integral (15) over the block-shaped volume V_S, the singularity at $R \to 0$ is correctly accounted for, and the typical components of the $\hat{\mathcal{D}}(\mathbf{r})$ tensor can be cast in the following form:

$$\mathcal{D}_{zz}(\mathbf{r}) = \frac{1}{8\pi} \sum_{i=p,m} \sum_{j=p,m} \sum_{k=p,m} [P_{ijk}^{(+)} - P_{ijk}^{(-)}], \qquad (23)$$

$$\mathcal{D}_{xy}(\mathbf{r}) = \frac{1}{8\pi} \sum_{i=p,m} \sum_{j=p,m} \sum_{k=p,m} [Q_{ijk}^{(+)} - Q_{ijk}^{(-)}], \qquad (24)$$

where

$$\begin{aligned}
P_{ijk}^{(\pm)} &= \arctan[X_i Z_k, (Y_j^2 + Z_k^2 \pm Y_j R_{ijk})], \\
Q_{ijk}^{(\pm)} &= \ln[X_i^2 Z_k^2 (Y_j^2 + Z_k^2 \pm Y_j R_{ijk})^2], \qquad (25) \\
R_{ijk} &= [X_i^2 + Y_j^2 + Z_k^2]^{1/2},
\end{aligned}$$

$$\begin{aligned}
X_p &= a_x + x, & Y_p &= a_y + y, & Z_p &= a_z + z, \\
X_m &= a_x - x, & Y_m &= a_y - y, & Z_m &= a_z - z.
\end{aligned}$$

In Eq. (25) the arctan ( ) function with *two* arguments is employed whose functional range is restricted to $-\pi \ldots +\pi$. The summation indices i, j, k assume the values p and m, yielding a total of 16 terms. They are clearly associated with the eight corners of the block. The remaining tensor components, beyond Eqs. (23,24), can be obtained by cyclic interchange of x, y, z. The diagonal components are in the range $0 < \mathcal{D}_{ii}(\mathbf{r}) < 1$ when $\mathbf{r}$ is inside a block-shaped sample. These results Eqs. (23,24) are in full agreement with the treatment by Durney et al. [5].

When the block-shaped sample is aligned with one of its axes along the field ($\theta = 0$), Eq. (23) is sufficient for the evaluation of $\omega(\mathbf{r})$. We determined the lineshapes $g_S(\omega - \omega_N)$ for a number of block-shaped samples, assuming the sensitivity to be uniform throughout ($S^2(\mathbf{r}) = 1$). The frequencies $\omega(\mathbf{r})$ were calculated for all positions of a three-dimensional grid with up to 10^6 points, and the $\omega(\mathbf{r})$ then sorted. Fig. 4 shows the results for square blocks of various heights. The frequency axis
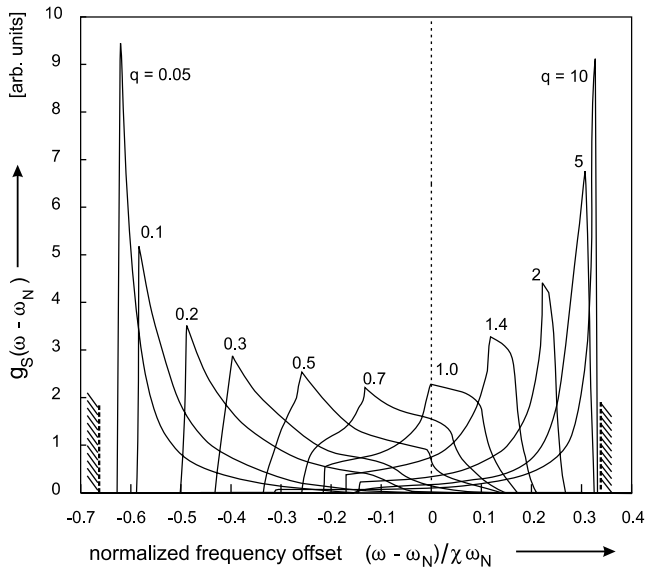
Fig. 4. Lineshapes $g_S(\omega - \omega_N)$ of samples in the form of square blocks ($a_x = a_y$) of various heights ($a_z = qa_x$). The parameter at the curves is the aspect ratio q.

is normalized by $\chi\omega_N$, assuming $\chi > 0$. For diamagnetic samples the frequency offset has the opposite sign. These spectra illustrate the influence of the BMS field. All lines are broadened, with sharp peaks, pronounced shoulders, and clearly defined upper and lower boundaries, ω_{max} and ω_{min}. The warped lineshapes are no computational artefacts but reflect the spatial structure of the demagnetizing fields $\mathbf{H}^{(S)}(\mathbf{r})$. Similar shapes are known from cylindrical samples [3]. In the limit of thin block-shaped samples ($q \ll 1$), demagnetization is strongest ($D_z \rightarrow 1$). The resulting lineshapes are shifted to lower frequencies by nearly the maximum possible value, $(2/3)\chi\omega_N$, relative to a spherical sample. Their peaks represent, in the sense of Fig. 3c, the 'core region' of fairly good field homogeneity in these thin samples. The high-frequency 'tails' result from the inhomogeneity caused by the four corner regions, where demagnetization is weakest and inhomogeneity strongest. For tall samples ($q \gg 1$) the situation is reversed. Their frequency spectra show nearly the maximum possible shift to higher frequencies, $(1/3)\chi\omega_N$. Their peaks result from the central regions of the samples, where demagnetization is weakest. Their low-frequency tails reflect the stronger demagnetization of the top and bottom regions. For $q = 1$ the sample is a cube. Its shape is closest to that of the sphere. Not surprisingly, the spectral shift is smallest here. The inhomogeneity is most pronounced at the eight corners, however, producing strongly asymmetric line broadening.

For a quantitative assessment of the BMS related line shifts and of the appropriate corrections, it is necessary to assign a characteristic frequency ω_S or ω_R to such a line of sample or reference, respectively. This is an ill-

defined problem due to the asymmetry of the lineshapes and, from an experimental viewpoint, due to the non-uniformity of practical sensitivity distributions $S^2(\mathbf{r})$. Therefore, ω_S or ω_R is chosen here pragmatically as the frequency ω_P of the prominent peak which exists in all these lineshapes. Likewise, despite of asymmetries, we will measure the width of a line simply at half maximum height. These definitions are reasonable because they emphasize the contribution by the 'core' region of the sample or reference volumes, where both the field and the sensitivity are most uniform. These regions are similar, in a broad sense, to the inscribed spheroid. In any block-shaped sample that spheroid occupies a fraction $\pi/6 \approx 0.52$ of the sample volume. Therefore, it is not surprising that the core region dominates, by its contribution to $\omega(\mathbf{r})$, the lineshape and produces the peak [3,4].

Fig. 5 shows for square block-shaped samples how the frequency ω_P of the peak depends on the aspect angle α. For comparison, the frequency shift for the spheroid that can be inscribed into the blocks is also shown (heavy broken line), as derived from Eq. (21). Near $\alpha_M = 43°$ the frequency shift of the square block vanishes, $\delta\omega_P = 0$. Accordingly, a block with the associated ratio of axes, $q_M = a_z/a_x \approx 0.94$, may be called a 'magic block' in analogy to the 'magic cylinder' [6,3]. This block is slightly shorter than a cube ($q = 1$), for which $\delta\omega_P = 0$ holds in the center. The difference may be understood from the definition of ω_P by the peak of $g(\omega - \omega_N)$ and from the structure of the field, whose component $\mathbf{H}_z^{(S)}$ increases from the center along the $\pm z$ directions, but decreases in all transverse directions.

We compare now in Fig. 5 the line shifts of square blocks with those of the inscribed spheroids. The peak frequency ω_P will be called ω_S from here on when it

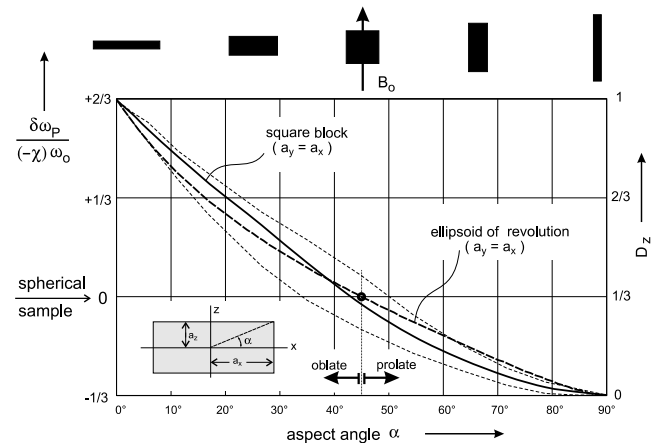
Fig. 5. Normalized shift of the peak frequency $\omega_S(\alpha)$ of samples having the shape of square blocks ($a_x = a_y$) with aspect angle α. The thin broken lines mark the half maximum height of the lines. For comparison the demagnetization $D_z(\alpha)$ for the inscribed spheroids ($a_x = a_y$) is reproduced from Fig. 3 (heavy broken line, right ordinate). The ordinates are labeled in the same way as in Fig. 3.

refers to the sample block. It is seen that the similarity suggested by Fig. 2c does indeed exist, but with moderate accuracy. Finite differences remain which can clearly be attributed to the influence of the corners of the block, outside the inscribed spheroid. The sign of the difference depends on α. For 'flat' samples ($\alpha < 40°$), the line shift $\delta\omega_S$ of the block is larger than $\delta\omega$ of the equivalent spheroid. Apparently, the demagnetizing field in the center of flat samples is stronger in a block than in its spheroid. For 'tall' samples ($\alpha > 40°$) the situation is reversed. In no case, however, does the line shift significantly exceed the width of the inhomogeneously broadened line. In other words, the (sharp) line of the inscribed spheroid is essentially always within the width of the asymmetrically broadened line of the block. In this sense the BMS induced line shift of a sample having the shape of a square block may well be approximated by that of the inscribed spheroid. The remaining uncertainty is less than 0.5 ppm.

This approximate determination of $\delta\omega$ works also with samples in the form of stripes of rectangular cross-section, arranged with their long axis normal to the main field, see Fig. 1a. This is the geometry typical in the measurement of lipid membranes supported by long glass slides [1]. Using Eq. (23) we calculated their demagnetizing fields in the limit $a_y \to \infty$. This was achieved by evaluating $\delta\omega(\mathbf{r})$ in the central region ($|y| < 0.1a_y$), where the field is fairly homogeneous, of moderately elongated samples ($a_y = 5a_x$). The results are summarized in Fig. 6. Again, the shifts $\delta\omega_S$ of the broadened spectra of the blocks are compared with the shifts of the sharp lines of the inscribed spheroids, i.e., of rods of the equivalent elliptical cross-section. They are spheroidal, their frequency shift follows from Eq. (14)
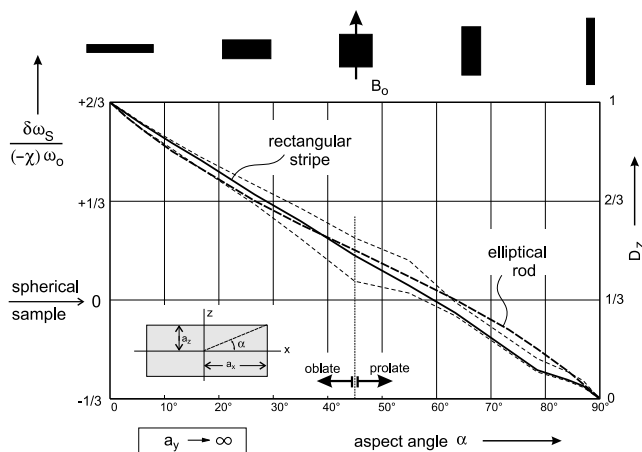

Fig. 6. Normalized shift of the peak frequency $\omega_S(\alpha)$ of samples having the shape of elongated blocks, oriented transversely to the field ($a_y \to \infty$), with aspect angle α. The thin broken lines mark the line widths at half maximum height. For comparison the demagnetization $D_z(\alpha)$ of the inscribed spheroidal samples ($a_y \to \infty$) is given (heavy broken line), which follows from Eq. (21).

and $D_z = q/(q - 1)$. As in Fig. 5, the comparison shows that blocks/stripes and spheroids differ only slightly in their line shifts. The difference is, again, roughly within the widths of the inhomogeneously broadened line. Compared with the spectra of square blocks (Fig. 5), the line broadening in stripes is less pronounced. It may be speculated that the stronger broadening in the square blocks results from the edges along the x direction whose influences are negligible in the long samples.

Approximation of the sample by the inscribed spheroid should work well also for a stack of circular disks, forming a cylindrical sample [8] that is suitable for magic angle-oriented sample spinning (MAOSS) [16]. The shape of such a cylinder is intermediate between a block and a spheroid (all having the same axes). Therefore, the field inhomogeneity, caused by the material outside the spheroid, should be less pronounced in the cylinder than in the block.

When the sample is tilted with respect to the main field we choose to describe $\mathbf{B}^{(o)}$ in the $\{x, y, z\}$ coordinate system of the sample. For simplicity we restrict the discussion to a rotation about the y axis, with tilt angle θ. Consequently $\mathbf{B}^{(o)}$ has x and z components, $\mathbf{B}^{(o)} = \mu_o H_o(\mathbf{x}^o \sin\theta + \mathbf{z}^o \cos\theta)$, where $\mathbf{x}^o$ and $\mathbf{z}^o$ are unit vectors. The generalization to a general orientation is straightforward, but lengthy. We now allow the samples to have uniaxially anisotropic susceptibility, but require them still to be homogeneous. In oriented membranes, the anisotropy is aligned with the z axis of Fig. 1, having a component $\chi_n(\mathbf{r})$ for fields normal to the membrane and $\chi_t(\mathbf{r})$ when they are tangential. Thus, a relevant example would be a layered block with negligibly thin glass layers. Eq. (7) now reads

$$\mathbf{M}(\mathbf{r}) = H_o[\chi_t(\mathbf{r}) \sin\theta \mathbf{x}^o + \chi_n(\mathbf{r}) \cos\theta \mathbf{z}^o]. \quad (26)$$

Using Eq. (8) the demagnetizing fields of the sample and of the Lorentz sphere are, respectively,

$$\mathbf{H}^{(S)}(\mathbf{r}) = -[\mathcal{D}_{xx}(\mathbf{r})\chi_t(\mathbf{r}) \sin\theta + \mathcal{D}_{xz}(\mathbf{r})\chi_n(\mathbf{r}) \cos\theta]\mathbf{x}^o H_o$$
$$- [\mathcal{D}_{yx}(\mathbf{r})\chi_t(\mathbf{r}) \sin\theta + \mathcal{D}_{yz}(\mathbf{r})\chi_n(\mathbf{r}) \cos\theta]\mathbf{y}^o H_o$$
$$- [\mathcal{D}_{zx}(\mathbf{r})\chi_t(\mathbf{r}) \sin\theta + \mathcal{D}_{zz}(\mathbf{r})\chi_n(\mathbf{r}) \cos\theta]\mathbf{z}^o H_o, \quad (27)$$

$$\mathbf{H}^{(L)}(\mathbf{r}) = -[\chi_t(\mathbf{r}) \sin\theta \mathbf{x}^o + \chi_n(\mathbf{r}) \cos\theta \mathbf{z}^o]H_o/3, \quad (28)$$

where $\mathcal{D}_{ij}(\mathbf{r})$ are the local components of the demagnetization tensor. Inserting Eqs. (27) and (28) into (12) yields the spatial distribution of the local frequency offset

$$\frac{\delta\omega(\mathbf{r})}{\omega_N} = \chi_n(\mathbf{r})\left[\frac{1}{3} - \mathcal{D}_{zz}(\mathbf{r})\right] + \sin^2\theta\left[\chi_t(\mathbf{r})\left[\frac{1}{3} - \mathcal{D}_{xx}(\mathbf{r})\right]\right.$$
$$\left. - \chi_n(\mathbf{r})\left[\frac{1}{3} - \mathcal{D}_{zz}(\mathbf{r})\right]\right]$$
$$- \sin\theta\cos\theta[\chi_t(\mathbf{r}) + \chi_n(\mathbf{r})]\mathcal{D}_{xz}(\mathbf{r}). \quad (29)$$

A tilted spheroidal sample is considered first. Here, the demagnetizing field is homogeneous. Therefore, the line is narrow but generally shifted from the frequency ω_N of a spherical sample. The demagnetization tensor is diagonal and reduces to the demagnetization factors, $\mathcal{D}_{xx}(\mathbf{r}) \to D_x$ and $\mathcal{D}_{zz}(\mathbf{r}) \to D_z$, given by Eq. (20). The y components play no role because the main field $\mathbf{H}^{(o)}$ is in the xz plane. The relative frequency offset resulting from BMS effects in the tilted spheroid is

$$\frac{\delta\omega(\theta)}{\omega_N} = \chi_n \left[\frac{1}{3} - D_z \right]$$
$$+ \sin^2\theta \left[\chi_t \left(\frac{1}{3} - D_x \right) - \chi_n \left(\frac{1}{3} - D_z \right) \right]. \quad (30)$$

The first bracket [ ] is the offset at $\theta = 0$, known from Eq. (14). The second bracket describes the variation of $\delta\omega$ when the sample is tilted, i.e., the apparent anisotropy. Both the material anisotropy $(\chi_t - \chi_n)$ and the shape anisotropy $(D_x - D_z)$ contribute here. For isotropic samples Eq. (30) simplifies to

$$\frac{\delta\omega(\theta)}{\chi\omega_N} = \left[\frac{1}{3} - D_z \right] + [D_z - D_x]\sin^2\theta. \quad (31)$$

Depending on the relative values of D_x and D_z, i.e., on the shape of the sample, an angle θ_o may exist at which $\delta\omega(\theta_o) = 0$. In particular, if the sample is symmetric about the z axis, we have $D_x = D_y$ and $D_z = 1 - 2D_x$. In that case $\theta_o \approx 54.7°$, identical to the 'magic angle'. This coincidence is fortunate for MAOSS applications, as it alleviates the need to compensate for BMS-induced effects [16]. This consideration applies to samples of cylindrical as well as square cross-sections.

In a tilted block-shaped sample the demagnetizing field is inhomogeneous, and generally the off-diagonal term $\mathcal{D}_{xz}(\mathbf{r})$ contributes in Eq. (29). Therefore, at any tilt angle θ, the spectral shift $\delta\omega(\mathbf{r})$ varies with positions $\mathbf{r}$ in a specific manner, different from that at $\theta = 0$. The broadened lineshape changes continuously as the sample is tilted. This is illustrated in Fig. 7 for a block of arbitrarily selected dimensions (long rectangular stripe normal to the field, $a_y \to \infty$, aspect ratio $q = a_x/a_z = 0.2$, aspect angle $\alpha \approx 11.3°$). Due to those changes in the lineshape it may seem that there is no simple description of the angular dependence of the line shift. However, the approximation by the inscribed spheroid which produces the line peak works here, too. At $\theta = 0°$ the peak is shifted to its extreme negative position, $\delta\omega_S/(\chi\omega_N) \approx -0.53$, in agreement with the demagnetizing factor $D_z \approx 0.86$ read from Fig. 6. When the sample is tilted to $\theta = 90°$ the x axis of the sample becomes aligned with the main field and the normalized shift of the peak reaches $+0.24$. In this orientation the sample may also be perceived as a rectangular stripe of aspect ratio $q_2 = 5$ in $\theta = 0°$ orientation. Again the shift is in agreement with the demagnetizing factor $D_z \approx 0.09$ gi-

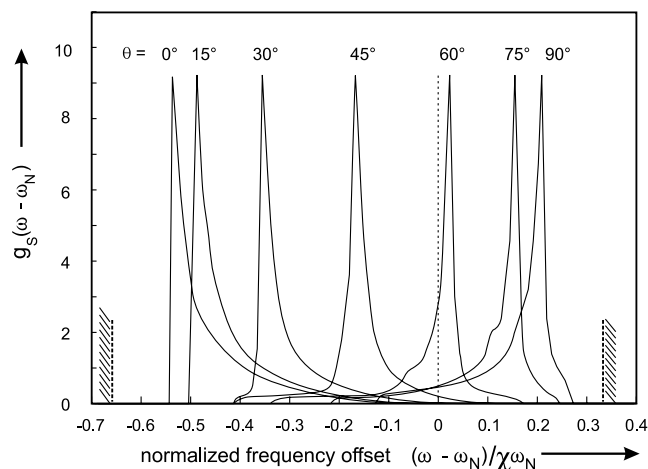Fig. 7. Normalized lineshapes $g_S(\omega - \omega_N)$ of one particular block-shaped sample ($a_z = 0.2a_x$ and $a_y \to \infty$) tilted through selected angles θ of rotation.

ven by Fig. 6 for $q_2 = 5$. At intermediate tilt angles the peak positions of Fig. 7 follow in good approximation the $\sin^2\theta$ variation predicted by Eq. (31) for a spheroidal sample inscribed into the block.

The symmetry just mentioned for a 90° tilt may be used to check the self-consistency of the numerical integration procedure. Generally, when a sample is tilted from any angular orientation θ_1 to a new orientation $\theta_2 = \theta_1 \pm 90°$, it becomes equivalent to another sample at orientation θ_1 but with $q_2 = 1/q_1$. In comparing such pairs of 'conjugated' samples no discrepancy is found in the frequency offsets $\delta\omega_S$ exceeding $\pm 0.02\chi\omega_N$. This corresponds to a chemical shift of ≈ 0.2 ppm. We therefore estimate that the accuracy of our calculations is of the same order.

4. BMS surface effects

For external referencing of stacks of membranes, the reference material is typically attached in the form of a thin slab directly onto the surface of the sample, as shown in Fig. 1a and as described in the accompanying paper [1]. To find the BMS related effects in that situation it is necessary to evaluate the demagnetizing field $\mathbf{H}^{(S)}(\mathbf{r})$ on the surface of the sample. For block-shaped samples this problem may be solved by a simple concept which will be discussed now.

From a practical point of view the key question with external referencing is the mutual influence which sample and reference material have on each other regarding line shifts and broadening. If the sample and reference compartments were measured separately, they would experience different BMS-related line shifts and broadenings, because they have different shapes. When they are brought into contact and are measured jointly, the demagnetizing field of either compartment modifies the

frequencies in the other one, causing additional shifts and broadenings. A first answer to this problem is possible in the limit where the volume of the reference material (including its container) is negligible compared to the sample volume. In that limit the demagnetizing influence of the reference on the sample is negligible, too. Conversely, however, the bulk sample block has profound influence on the frequency of the thin reference. To find that influence, the demagnetizing field must be determined for the combination of both compartments, and from it the spectra Eq. (22) must be evaluated separately for either compartment.

When the sample block with the attached external reference is aligned with the main field ($\theta = 0°$) as in Fig. 1a, the demagnetizing field $\mathbf{H}^{(S)}(\mathbf{r}_t)$ at the top surface $z = +a_z$ can be found from the model which postulates 'magnetic charges' $\sigma(\mathbf{r})$ as the sources of $\mathbf{H}^{(S)}(\mathbf{r})$. For simplicity we assume that the susceptibilities of sample and reference are equal. Consequently there is a homogeneous positive charge density $\sigma^{(+)} = \chi H_o$ on the top surface of the sample block, and a corresponding negative charge density $\sigma^{(-)} = -\chi H_o$ on the bottom. The field $\mathbf{H}^{(S)}(\mathbf{r})$ resulting from these charges is sketched in Fig. 8a. It may be viewed as the superposition of two contributions, produced separately by $\sigma^{(+)}$ and $\sigma^{(-)}$, see Fig. 8b and c. Immediately adjacent to either layer of charges the fields of these charges are homogeneous, their magnitude being $|\mathbf{H}^{(S)(+)}(\mathbf{r})| = |\sigma|/2$. These field regions dominate the demagnetization in the reference compartment on the top of the block. The reference material 'sees' such a homogeneous field produced by $\sigma^{(+)}$ of the combined block, as shown in Fig. 8b. The negative charges $\sigma^{(-)}$ are farther away. They produce a weaker and generally inhomogeneous field $\mathbf{H}^{(S)(-)}(\mathbf{r}_t)$, sketched in Fig. 8c. That field can be specified more precisely by adding a mirror image of the sample on top of the sample. Sample and image form a new block which will be dubbed 'M-block'. It has the same cross-section ($2a_x \times 2a_y$) as the actual sample, but its height ($4a_z$) is doubled, see Fig. 8d. Therefore, top and bottom of that M-block carry the same charge densities $\sigma^{(+)}$ and $\sigma^{(-)}$ as the original block.

In the center plane of the M-block the charges $\sigma^{(-)}$ produce a field which is exactly the required $\mathbf{H}^{(S)(-)}(\mathbf{r}_t)$. A second, symmetrical contribution comes from the charges at the top of the M-block. Therefore, the z component of the required field $\mathbf{H}^{(S)(-)}(\mathbf{r}_t)$ is half of the field in the center plane of the M-block. According to this construction, the spectral offset of the external reference compartment can be expressed as

$$\frac{\delta\omega_R(\mathbf{r}_t)}{\chi\omega_N} = \frac{1}{3} - \frac{1}{2}[1 + \mathcal{D}_{zz,\text{M-block}}(\mathbf{r}_c)]. \tag{32}$$

Here, $\mathbf{r}_c$ denotes the center plane of the M-block, coincident with the top surface $\mathbf{r}_t$ of the combination of sample and reference. Approximating now the field in the M-block by the field in the inscribed M-spheroid, we arrive at

$$\frac{\delta\omega_R(\theta = 0°)}{\chi\omega_N} = -\frac{1}{2}\left[\frac{1}{3} + D_z(a_x, a_y, 2a_z)\right] \tag{33}$$

for the BMS-related line shift of the reference compartment. Here, (a_x, a_y, a_z) are the semi-axes of the sample block and D_z is given by Eq. (20). In approximating the M-block by its equivalent spheroid, similar limitations apply, of course, as discussed above.

To illustrate this result we consider a sample having the shape of a cube. At its center $D_x = D_y = D_z = 1/3$, and Eq. (13) shows that the local line shift vanishes there. The same had been concluded above for the peak of the broadened line of the entire sample. For a thin external reference layer placed onto the top surface, however, Eq. (33) yields a normalized shift of -0.254, where $D_z(1, 1, 2) \approx 0.174$ is obtained from Eq. (20) or (21). If the thin reference layer were measured by itself, without the cube, $D_z(1, 1, 0) \rightarrow 1$ would apply and a normalized shift of -0.667 would be found. The difference of these shifts, $+0.413$, must be viewed as the influence which the bulk sample has on the reference layer.

A tilted sample with attached reference layer is treated again in the $\{x, y, z\}$ system of the sample block, by rotating the direction of the main field $\mathbf{B}^{(o)}$ about the y axis. We start by considering the case $\theta = 90°$, where $\mathbf{B}^{(o)}$ lies along the x direction, tangential to the reference layer, and thereafter discuss the case of a general tilt angle. For $\theta = 90°$, the field at the surface ($z = +a_z$) of the joint block can be found by a similar argument as above, considering an M-block which has twice the height of the sample. We are interested only in the x component of $\mathbf{H}^{(S)}(\mathbf{r}_t)$, parallel to $\mathbf{B}^{(o)}$. By adding the second half of the M-block, this x component is doubled, and the reference layer becomes the center plane of the M-block. As there are no charges at the plane $z = +a_z$, the spectral offset at points $\mathbf{r}_t$ in the reference compartment can be expressed simply as

$$\frac{\delta\omega_R(\mathbf{r}_t)}{\chi\omega_N} = \frac{1}{3} - \frac{1}{2}\mathcal{D}_{xx,\text{M-block}}(\mathbf{r}_c). \tag{34}$$
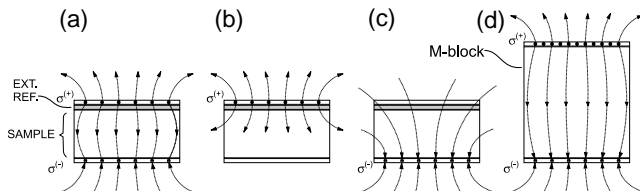

Fig. 8. (a) The demagnetizing field $\mathbf{H}^{(S)}$ of a block-shaped sample with attached reference layer may be understood as being generated by fictive 'magnetic surface charges'. Assuming $\chi_R = \chi_S > 0$, positive charges exist on the top surface of the reference layer, producing the field component shown in (b), and negative charges at the bottom produce the component shown in (c). In the reference layer, the field component from the negative charges is equal to half the field in the center plane of the M-block, shown in (d).

Approximating again the field in the M-block by the field in the inscribed M-spheroid yields

$$\frac{\delta\omega_R(\theta = 90°)}{\chi\omega_N} \approx \frac{1}{3} - \frac{1}{2}D_x(a_x, a_y, 2a_z). \quad (35)$$

For the cubic sample considered above, we have $D_x(1,1,2) \approx 0.413$ and obtain a normalized shift of $+0.127$. This may be compared with a shift of $+0.333$ if the reference layer were measured by itself with an x-directed main field. The difference, -0.206, is the influence of the sample cube on the reference layer when tilted to $\theta = 90°$.

For a general tilt angle θ, the $\mathbf{B}^{(o)}$ field has components along both the z and x directions. For either case the demagnetizing field is known. By linear superposition of these fields with weighting factors $\sin\theta$ and $\cos\theta$ we obtain from Eqs. (32,34) the normalized spectral shifts for a surface position $\mathbf{r}_t$ on a general sample

$$\frac{\delta\omega_R(\mathbf{r}_t)}{\chi\omega_N} = -\frac{1}{2}\left[\frac{1}{3} + \mathcal{D}_{zz,\text{M-block}}(\mathbf{r}_c)\right] + \frac{\sin^2\theta}{2}$$
$$\times [1 + \mathcal{D}_{zz,\text{M-block}}(\mathbf{r}_c) - \mathcal{D}_{xx,\text{M-block}}(\mathbf{r}_c)]. \quad (36)$$

Here again, $\mathbf{r}_t$ and $\mathbf{r}_c$ denote the same point, but refer to different blocks. The second bracket is the local anisotropy. As it depends on the position $\mathbf{r}_t$ at the surface, the reference spectrum changes not only its offset $\delta\omega_R$, but also its lineshape, when the sample and attached reference are jointly tilted. It is not possible, therefore, to express the angular dependence in a precise, general form. However, when we approximate the spectrum of the M-block by the inscribed spheroid, we find from Eqs. (33) and (35), independent of position in the reference compartment,

$$\frac{\delta\omega_R(\theta)}{\chi\omega_N} \approx -\frac{1}{2}\left[\frac{1}{3} + D_z(a_x, a_y, 2a_z)\right] + \frac{\sin^2\theta}{2}$$
$$\times [1 + D_x(a_x, a_y, 2a_z) - D_z(a_x, a_y, 2a_z)]. \quad (37)$$

The first bracket is again the offset at $\theta = 0°$. The second one represents an anisotropy of the reference frequency which must be attributed to the presence of the sample compartment at one side of the reference compartment.

The concept described above may be generalized to a situation where the susceptibilities of sample χ_S and reference χ_R are different. If, in that case, $\theta = 0$, an additional charge density $\sigma^{(i)} = (\chi_S - \chi_R)H_o$ must be accounted for at the interface between sample block and reference layer. The field in the reference layer is now the sum of tree terms. The two fields produced by $\sigma^{(+)}$ and $\sigma^{(i)}$ are essentially homogeneous. The third term results from $\sigma^{(-)}$ at the bottom of the block and is inhomogeneous. Its z component can again be obtained by means of an M-block, having the susceptibility χ_S and the height $4a_z$. Instead of Eq. (32) we find

$$\frac{\delta\omega_R(\mathbf{r}_t)}{\omega_N} = \frac{1}{3} - \frac{\chi_S}{2}\left[2\frac{\chi_R}{\chi_S} - 1 + \mathcal{D}_{zz,\text{M-block}}(\mathbf{r}_c)\right].$$

5. Anisotropy of the layered block

A sample block assembled as a stack of coated glass slides [1,8,9] shows anisotropic behavior on three scales. First, there is *macroscopic* anisotropy if the axes a_x, a_y, a_z of the block have different lengths and/or if the material of the block is anisotropic. These effects have been discussed above. Second, on a *microscopic* scale, anisotropy may result from the layered structure because the magnetic susceptibility χ_G of the glass is generally different from the that of the lipid. Third, anisotropy exists on a *molecular* scale because the lipid bilayers spontaneously orient themselves parallel to the glass surface. The susceptibility χ_L of the lipid material is a tensor, therefore, with a component χ_{Lt} for a magnetic field tangential to the surface and χ_{Ln} when the field is normal. To discuss the role of the layered structure we repeat the calculations following Eq. (11), including now the anisotropy at microscopic and molecular scales.

We start by treating the layered block as an anisotropic, though homogeneous 'mean' magnetic material, exhibiting the average magnetization, $\mathbf{M}_M(\mathbf{r}) = \beta_G\mathbf{M}_G(\mathbf{r}) + \beta_L\mathbf{M}_L(\mathbf{r})$. Here, β_G and $\beta_L = 1 - \beta_G$ are the volume filling factors of glass and lipid, respectively. Denoting the thicknesses of these layers by w_G and w_L, we have $\beta_k = w_k/(w_G + w_L)$ for $k = G, L$. On the macroscopic scale, therefore, a block of this mean material behaves magnetically identical to the block with layered structure, $\mathbf{B} = (1 + \chi_M)\mathbf{H}$ with a tensor χ_M. The definition of this mean material is reasonable if the thicknesses of the layers are small enough that the fields may be considered homogeneous across each layer. For the stack of coated glass slides this assumption is justified throughout most of the volume except for a narrow region at the four side walls in Fig. 1a whose width is comparable to the thickness of the glass slides [1]. We use this χ_M to calculate from Eq. (30) that part of the line shift which results from the block- or spheroid-shaped geometry of a sample.

On the microscopic scale, we consider the lipid layer embedded in the mean material. The field $\mathbf{H}_L^{(L)}(\mathbf{r})$ inside the lipid is found from the field $\mathbf{H}_M^{(L)}(\mathbf{r})$ in the mean material by taking into account the 'local demagnetization' factor D_{loc} according to the orientation of the layers.

To determine χ_M we split all fields into their components normal and tangential to the layers. In the lipid, $\mathbf{B}_L = \mathbf{B}_{Ln} + \mathbf{B}_{Lt}$ and $\mathbf{H}_L = \mathbf{H}_{Ln} + \mathbf{H}_{Lt}$. Continuity relations at the interfaces between glass and lipid require $\mathbf{B}_{Mn} = \mathbf{B}_{Ln} = \mathbf{B}_{Gn}$ and $\mathbf{H}_{Mt} = \mathbf{H}_{Lt} = \mathbf{H}_{Gt}$. The components of the mean susceptibility are defined through $\mathbf{B}_{Mt} = (1 + \chi_{Mt})\mu_o\mathbf{H}_{Mt}$ and $\mathbf{H}_{Mn} = (1 - \chi_{Mn})\mathbf{B}_{Mn}/\mu_o$, assuming that all susceptibilities are small. These relations are consistent if we choose

$$\chi_{Mn} = \beta_G\chi_G + \beta_L\chi_{Ln}, \quad (38)$$

$$\chi_{Mt} = \beta_G\chi_G + \beta_L\chi_{Lt}. \quad (39)$$

The field $\mathbf{H}_L^{(S)}$ at the site of the spin consist generally of three contributions: the demagnetizing field $\mathbf{H}_{D,M}^{(S)}$ of the mean block, the local demagnetizing field $\mathbf{H}_{D,\mathrm{loc}}^{(S)}$ resulting from the susceptibility mismatch between the mean material and the lipid layer, and the field $\mathbf{H}_L^{(L)}$ of the Lorentz sphere. Considering first the situation $\theta = 0°$, when the field is normal to the layers, only the n-components of the susceptibilities enter. We have $\mathbf{H}_{D,M}^{(S)} = -\chi_{Mn} D_z H_o$ according to Eq. (30), and $D_{\mathrm{loc}} = 1$ in the second contribution. If the layered block is rotated to $\theta = 90°$ the t-components matter, and $\mathbf{H}_{D,M}^{(S)} = -\chi_{Mt} D_x H_o$. In this orientation $D_{\mathrm{loc}} = 0$. In this way we obtain the normalized line shift of a spin in the lipid layer of a layered sample, tilted by θ about the y axis, in the approximation of the inscribed spheroid

$$\frac{\delta\omega(\theta = 0°)}{\omega_N} = \chi_{Mn}\left(\frac{1}{3} - D_z\right) - \frac{2}{3}(\chi_{Ln} - \chi_{Mn}), \qquad (40)$$

$$\frac{\delta\omega(\theta = 90°)}{\omega_N} = \chi_{Mt}\left(\frac{1}{3} - D_x\right) + \frac{1}{3}(\chi_{Lt} - \chi_{Mt}). \qquad (41)$$

For intermediate angles of rotation, the frequency shift interpolates according to $\sin^2\theta$ between these limits. This can be concluded generally from the derivation leading to Eq. (29). The first terms on the right hand sides above are the shape anisotropies which appeared already in Eq. (30). The additional terms result from the layered structure. They are proportional to the susceptibility mismatch between the lipid layer and the 'mean' material defined by Eqs. (38,39). In many practical situations the lipid filling factor is small, $\beta_L \ll 1$, and the 'mean' material is essentially equal to the glass used as substrate. If, moreover, the lipid were magnetically isotropic, a 'structural' anisotropy of $(\delta\omega_{90} - \delta\omega_0)/\omega_N = (\chi_L - \chi_G)$ would be measured between $\theta = 0°$ and $\theta = 90°$, in addition to any shape anisotropy present. Inserting here typical susceptibilities, $\chi_L \approx -8 \times 10^{-6}$ and $\chi_G \approx -12 \times 10^{-6}$, yields a value of $\approx 4\,\mathrm{ppm}$ for the structural anisotropy and shows the significance of this effect.

6. Conclusions

A theoretical analysis has been performed of the BMS induced shift and broadening of NMR lines in block-shaped samples. The latter are typically obtained by stacking a number of thin glass slides which support uniaxially oriented biomembranes and a flat reference layer attached on top. For their preparation and for internal and external referencing of their spectra, a detailed understanding of these BMS effects is helpful. The key results are:

- Depending on the aspect ratio of the block, the BMS induced shift may be positive or negative. The broadening is asymmetric, with widely varying lineshapes.

- Sample and reference lines experience different shifts, $\delta\omega_S$ and $\delta\omega_R$. Their difference is the correction which must be applied to a measured chemical shift.
- Explicit determination of the lineshape and shift is possible by calculating from Eq. (23) the demagnetizing field at a large number of points in the block, and then sorting the associated frequencies into a histogram.
- Despite asymmetry of broadening, the resulting lines generally have a pronounced peak.
- The spectral position of that peak, i.e., the line shift caused by BMS effects in the *volume* of the sample block, is close to that of the sharp line which would result for the spheroid inscribed in the block. When an axis of the block is aligned parallel to the field, this shift in the spheroid is readily found from the ratios of its semi-axes, using Eq. (20) or (21), or from Fig. 5 (square blocks) or Fig. 6 (long stripes).
- A heuristic explanation of this volume effect is that the inscribed spheroid occupies more than half of the block volume and is dominant, therefore, in the spectrum. The demagnetizing field of the eight corner regions impairs the field homogeneity in the spheroid, however, thus broadening its line.
- For a block tilted by θ about one of its axes, the line position interpolates as $\sin^2\theta$ between the two extreme orientations $\theta = 0°$ and $\theta = 90°$.
- When a substrate material (glass) is used to support the oriented membranes, the apparent anisotropy has contributions from the shape of the sample, from the material anisotropy $\chi_{Ln} - \chi_{Lt}$ of the lipid, and from the susceptibility mismatch between glass and lipid, depending also on the filling factor β_L of the lipid.
- For a thin external reference layer, attached to one *surface* of the block, the BMS induced shift can be found by evaluating the volume effect in a block doubled about that surface.

References

[1] R.W. Glaser, A.S. Ulrich, Susceptibility corrections in solid state NMR experiments with macroscopically oriented membrane samples. Part I: Applications, J. Magn. Reson. 164 (2003) 104–114.

[2] G. Mozurkewich, H.I. Ringermacher, D.I. Bolef, Effect of demagnetization on magnetic resonance line shapes in bulk samples: application to tungsten, Phys. Rev. B 20 (1979) 33–38.

[3] T.M. Barbara, Cylindrical demagnetization fields and microprobe design in high-resolution NMR, J. Magn. Reson. A 109 (1994) 265–269.

[4] A. Kubo, T. Spaniol, T. Terao, The effect of bulk magnetic susceptibility on solid state NMR spectra of paramagnetic compounds, J. Magn. Reson. 133 (1998) 330–340.

[5] C.H. Durney, J. Bertolina, D.C. Allion, R. Christman, A.G. Cutillo, A.H. Morris, S. Hashemi, Calculation and interpretation of inhomogeneous line broadening in models of lungs and

other heterogeneous structures, J. Magn. Reson. 85 (1989) 554–570.

[6] C.S. Springer, Physicochemical principles influencing magneto-pharmaceuticals, in: R.J. Gillies (Ed.), NMR in Physiology and Biomedicine, Academic Press, Orlando, FL, 1994, pp. 75–99.

[7] S.N. Hwang, F.W. Wehrli, The calculation of the susceptibility-induced magnetic field from 3D NMR images with applications to trabecular bone, J. Magn. Reson. B 109 (1995) 126–145.

[8] O. Soubias, O. Saurel, V. Réat, A. Milon, High resolution ^{13}C NMR spectra on oriented lipid bilayers: from quantifying the various sources of line broadening to performing 2D experiments with 0.2–0.3 ppm resolution in the carbon dimension, J. Biomol. NMR 24 (2002) 15–30.

[9] J. Salgado, S.L. Grage, L.H. Kondejewski, R.S. Hodges, R.N. McElhaney, A.S. Ulrich, Membrane-bound structure and alignement of the antimicrobial β-sheet peptide gramicidin S derived

from angular and distance constraints by solid-state ^{19}F-NMR, J. Biomol. NMR 21 (2001) 191–208.

[10] *Note*: Some authors define $B = \tilde{H} + 4\pi\tilde{M}$ *and* $\mu = 1 + 4\pi\tilde{\chi}$, using alternative variables $\tilde{H}$, $\tilde{M}$, and $\tilde{\chi} = \chi/4\pi$ which differ by a factor 4π. In that notation $\tilde{H}^{(S)} = -\tilde{D}\tilde{M} = -\tilde{D}\tilde{\chi}\tilde{H}$ where $\tilde{D} = 4\pi D$ and $\sum \tilde{D}_{ii} = 4\pi$.

[11] K. Simonyi, Theoretische Elektrotechnik, VEB Deutscher Verlag der Wissenschaften, Berlin, 1979.

[12] J.A. Osborn, Demagnetizing factor of the general ellipsoid, Phys. Rev. 67 (1945) 351–357 (see [10]).

[13] MAPLE, Waterloo, Ont., Canada.

[14] MATHEMATICA, Champaign, IL, USA.

[15] MATLAB, Natick, MA, USA.

[16] C. Glaubitz, A. Watts, Magic angle-oriented sample spinning (MAOSS): a new approach toward biomembranes studies, J. Magn. Reson. 130 (1998) 305–316.